# RNA nuclear export is blocked by poliovirus 2A protease and is concomitant with nucleoporin cleavage

**Alfredo Castelló*, José M. Izquierdo, Ewelina Welnowska and Luis Carrasco‡**

Centro de Biología Molecular 'Severo Ochoa' (CSIC-UAM), C/Nicolás Cabrera, 1. Universidad Autónoma de Madrid. Cantoblanco, 28049 Madrid, Spain

*Present address: European Molecular Biology Laboratory (EMBL), Meyerhofstrasse 1, 69117 Heidelberg, Germany
‡Author for correspondence (lcarrasco@cbm.uam.es)

*Accepted 12 August 2009*
*Journal of Cell Science 122, 3799-3809 Published by The Company of Biologists 2009*
*doi:10.1242/jcs.055988*

## Summary

**Cytopathic viruses have developed successful strategies to block or, at least, to attenuate host interference with their replication. Here, we have analyzed the effects of poliovirus 2A protease on RNA nuclear export. 2A protease interferes with trafficking of mRNAs, rRNAs and U snRNAs from the nucleus to the cytoplasm, without any apparent effect on tRNA transport. Traffic of newly produced mRNAs is more strongly affected than traffic of other mRNAs over-represented in the cytoplasm, such as mRNA encoding β-actin. Inhibition of RNA nuclear export in HeLa cells expressing 2A protease is concomitant with the cleavage of Nup98, Nup153, Nup62 and their subsequent subcellular redistribution. The expression of an inactive 2A protease failed to interfere with RNA nuclear export. In addition, other related proteases, such as poliovirus 3C or foot and mouth disease virus $L^{pro}$ did not affect mRNA distribution or Nup98 integrity. Treatment of HeLa cells with interferon (IFN)-γ increased the relative amount of Nup98. Under such conditions, the cleavage of Nup98 induced by 2A protease is partial, and thus IFN-γ prevents the inhibition of RNA nuclear export. Taken together, these results are consistent with a specific proteolysis of Nup98 by 2A protease to prevent de novo mRNA traffic in poliovirus-infected cells.**

Supplementary material available online at
http://jcs.biologists.org/cgi/content/full/122/20/3799/DC1

Key words: 2A protease, RNA nuclear export, Nucleoporin, Interferon, Gene expression control

## Introduction

Poliovirus (PV) is a member of the Enterovirus genus in the *Picornaviridae* family and is the causative agent of poliomyelitis. This virus contains a single positive-strand RNA as genome, which encodes a large polyprotein that is cleaved to generate the mature and functional proteins. This proteolytic processing is exerted by two virus-encoded proteases known as $2A^{pro}$ and $3C^{pro}$ (Seipelt et al., 1999), which have been also implicated in the inhibition of host gene expression in infected cells (Lloyd, 2006; Weidman et al., 2003). Both proteases induce the blockade of protein synthesis by cleaving eukaryotic translation initiation factors (eIFs). $2A^{pro}$ hydrolyzes eIF4GI and eIF4GII, whereas $3C^{pro}$ cleaves poly(A)-binding protein (PABP) (Lloyd, 2006). PV RNA contains an internal ribosome entry site (IRES) that ensures translation despite eIF4G cleavage (Martinez-Salas and Fernandez-Miragall, 2004). $2A^{pro}$ and $3C^{pro}$ also target some nuclear factors, including several transcription factors (Weidman et al., 2003) and, in the case of $2A^{pro}$, the structural component of small nuclear ribonucleoproteins (snRNPs) gemin-3, which is implicated in eukaryotic intron removal mediated by the spliceosome machinery (Almstead and Sarnow, 2007).

The traffic of biological molecules between the nucleus and the cytoplasm occurs through a macromolecular structure known as the nuclear pore complex (NPC). The metazoan NPC is composed of multiple copies of ~30 different proteins, known as nucleoporins (Nup). NPC forms large structures (~125 MDa) embedded in the nuclear membrane and generates a channel through the nuclear envelope. Eight filaments of ~50 nm project into the cytoplasm and a basket-like structure extends 100 nm into the nucleoplasm. These NPC extensions might function as initial cargo-docking sites during nuclear-cytoplasmic transport (Cullen, 2003; Kohler and Hurt, 2007). Some viruses severely damage NPC architecture, which leads to the inhibition of protein trafficking between the nucleus and the cytoplasm (Belov et al., 2004; Gustin and Sarnow, 2001; Gustin and Sarnow, 2002; Park et al., 2008; Porter and Palmenberg, 2009), inhibition of RNA export from the nucleus (Her et al., 1997; Satterly et al., 2007), and, in some instance, an increase of the nuclear membrane permeability at later times post-infection (Belov et al., 2004; Lidsky et al., 2006). Here, we report that PV $2A^{pro}$ induces alterations in the NPC, which inhibits nuclear export of U snRNA, rRNA and mRNA but not that of tRNAs. The inhibition of trafficking of de-novo-synthesized mRNAs occurs early after $2A^{pro}$ expression, suggesting that this protease could prevent host responses to viral infection.

## Results

### PV $2A^{pro}$ alters nuclear export of mRNAs, U snRNAs and rRNAs but not tRNAs

Translation of newly synthesized mRNAs is blocked by PV $2A^{pro}$ earlier than that of mRNAs involved in ongoing protein synthesis (Castello et al., 2006a; Novoa and Carrasco, 1999), suggesting that this protease might interfere with an early step of gene expression. Previous reports showed that the NPC was altered in PV-infected cells (Belov et al., 2004; Gustin and Sarnow, 2001; Gustin and

Sarnow, 2002; Park et al., 2008). Thus, we investigated the impact of PV $2A^{pro}$ on the export of cellular RNAs from nucleus to cytoplasm. First, we analyzed the cellular distribution of de-novo-synthesized luciferase mRNAs in Tet-off HeLa X1/5 cells that express PV $2A^{pro}$ (Castello et al., 2006a). Luciferase mRNA synthesis was induced by removal of tetracycline (Tet) from the culture medium (Novoa and Carrasco, 1999), and the expression of PV $2A^{pro}$ was achieved by the electroporation of 1 or 9 μg of an in-vitro-synthesized mRNA that contained the encephalomyocarditis virus (EMCV) IRES followed by the PV $2A^{pro}$ coding sequence (IRES-2A mRNA) (Castello et al., 2006a). At 8 hours post-electroporation (hpe), luciferase activity and the integrity of eIF4GI and eIF4GII were estimated.

Luciferase activity decreased by about 90% in $2A^{pro}$-expressing cells compared with control cells, irrespective of the IRES-2A mRNA dose employed (supplementary material Fig. S1A). However, 9 μg IRES-2A mRNA was required to strongly inhibit ongoing β-actin protein synthesis (supplementary material Fig. S1B). As expected, eIF4GI was proteolyzed in cells electroporated with 1 μg IRES-2A mRNA, whereas eIF4GII remained intact. By contrast, electroporation of 9 μg IRES-2A mRNA induced total cleavage of both eIF4GI and eIF4GII (supplementary material Fig. S1C). To determine whether the decrease in luciferase synthesis in $2A^{pro}$-expressing cells was due to an inhibition of RNA nuclear export, nuclear and cytoplasmic fractions were prepared from the different electroporated cells. Total RNA was then isolated from each subcellular fraction and the steady-state levels of luciferase or β-actin mRNAs were quantified by real-time reverse transcriptase (RT)-PCR. The effectiveness of fractionation was checked by western blot analysis against a cytoplasmic protein such as α-tubulin or a nuclear protein such as poly-ADP-ribose polymerase (PARP).

As expected, α-tubulin was present only in the cytoplasmic fraction, whereas PARP was only detected in the nuclear fraction (supplementary material Fig. S1D). Interestingly, the ~80 KDa cleavage product related to caspase-3-mediated cleavage of PARP was not detected in either case (supplementary material Fig. S1D), suggesting that apoptosis was not induced by the viral protease at these particular times and doses. The total amount of luciferase and β-actin mRNAs was similar in control and in $2A^{pro}$-expressing cells, suggesting that transcription was not hampered by the PV protease (Fig. 1A). The distribution of β-actin mRNA in nuclear and cytoplasmic fractions was not significantly altered in $2A^{pro}$-expressing cells as compared with that in control cells (Fig. 1B). The cytoplasmic to nuclear (C/N) ratio of this mRNA was

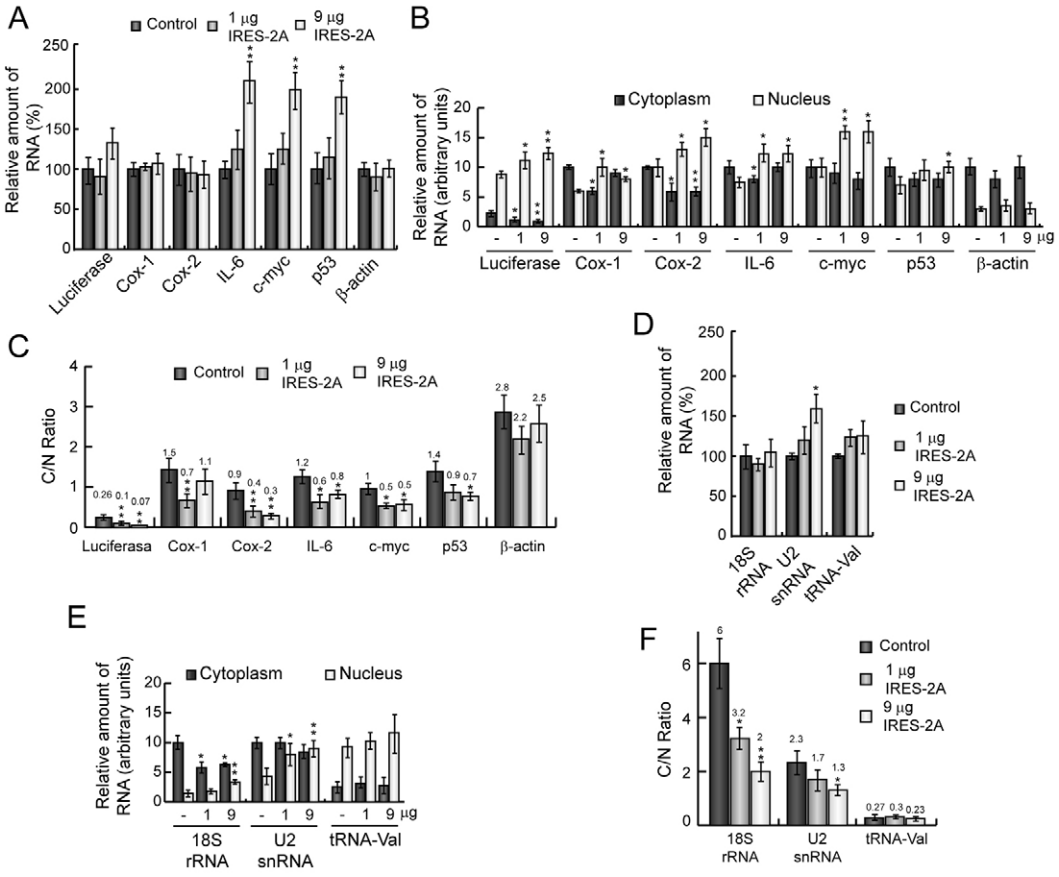


**Fig. 1.** Nuclear-cytoplasmic distribution of cellular mRNAs, 18S rRNA, U2 snRNA and tRNA-val in PV 2A-expressing cells. HeLa X1/5 cells, incubated with 20 ng/ml Tet, were electroporated with either 1 or 9 μg IRES-2A mRNA, or with transcription buffer as a control. During electroporation, Tet was removed from the culture medium. Total, nuclear and cytoplasmic fractions were obtained in each case at 8 hpe. Luciferase, COX-1, COX-2, IL-6, IL-2, c-myc, p53 and β-actin mRNAs and 18S rRNA, U2 snRNA and tRNA-val were quantified in each fraction by real-time RT-PCR using specific oligonucleotides and Taqman probes. (A) Relative amount of each mRNA in the total fraction from control cells (black bars) or cells electroporated with 1 (grey bars) or 9 μg (white bars) IRES-2A mRNA. (B) Relative quantitation of each mRNA in the nuclear and cytoplasmic fractions. (C) C/N ratio calculated for each mRNA in the presence or absence of $2A^{pro}$. (D) Relative level of 18S rRNA, U2 snRNA and tRNA-Val in the total fraction of control (black bars) or 2A-expressing cells (grey and white bars). (E) Relative quantitation of 18S rRNA, U2 snRNA and tRNA-Val in nuclear and cytoplasmic fractions. (F) C/N ratio calculated for 18S rRNA, U2 snRNA and tRNA-Val. Values are means ± s.d. $*P<0.05$, $**P<0.01$ compared with control, calculated using the Student's *t*-test.

approximately 2-3 in each case (Fig. 1C). By contrast, the distribution of luciferase mRNA was strongly altered in $2A^{pro}$-expressing cells. Whereas the amount of luciferase mRNA in the cytoplasmic fraction decreased, it increased in the nuclear fraction (Fig. 1B,C). It is worth noting that the C/N ratio of luciferase mRNA was 9.2% that of β-actin in control cells (Fig. 1C). This could be because luciferase mRNA is capped and polyadenylated by host machinery, but it is not spliced. Hence, this mRNA might be exported by an inefficient pathway that involves the CRM1 transporter (Cullen, 2003; Kohler and Hurt, 2007). The C/N ratio of luciferase mRNA decreased from 0.26 to ~0.1, and to ~0.07 in cells electroporated with 1 μg and 9 μg IRES-2A mRNA, respectively (Fig. 1C). These results suggest that nuclear export of de-novo-synthesized mRNAs is more sensitive to $2A^{pro}$ than the export of mRNAs that are over-represented in the cytoplasm.

To rule out the possibility that the CRM1-mediated export pathway could be more susceptible to $2A^{pro}$ activity, the subcellular distribution of different endogenous spliced mRNAs involved in immunological responses against pathogens [cyclooxygenase (COX)-1, COX-2, interleukin (IL)-2, IL-6], in cell survival and death (p53) and in cell proliferation (c-myc) was analyzed in these cells. As expected, the most abundant mRNA in the total fraction of control cells was β-actin, whereas IL-2 mRNA was not detected (supplementary material Fig. S1E). Steady-state levels of IL-6, c-myc and p53 mRNAs increased in cells electroporated with IRES-2A mRNA in a dose-dependent manner (Fig. 1A). Probably, the presence of PV $2A^{pro}$ induced a host gene response. Similarly to the luciferase mRNA, relative levels of COX-1, COX-2, IL-6, c-myc and p53 mRNAs increased in the nuclear fraction and decreased or, at least, were maintained in the cytoplasmic fraction of cells electroporated with IRES-2A mRNA (Fig. 1B). Consequently, the C/N ratio of each mRNA diminished in $2A^{pro}$-expressing cells in all cases (Fig. 1C). Therefore, $2A^{pro}$ not only interferes with the nuclear export of luciferase mRNA but also inhibits the traffic of spliced mRNAs. β-actin appears to be insensitive to $2A^{pro}$, although the contribution of the half-life of each mRNA might account, at least in part, for this effect.

rRNAs, snRNAs and tRNAs are exported to the cytoplasm by other pathways than those used to transport mRNAs. To analyze the functionality of these RNA export pathways in $2A^{pro}$-expressing cells, the distribution of 18S rRNA, U2 snRNA and tRNA-Val were studied. Expression of $2A^{pro}$ did not affect the total relative amount of 18S rRNA or tRNA-Val but moderately increased the level of U2 snRNA (~1.5-fold) (Fig. 1D). Looking at the subcellular distribution, 18S rRNA decreased in the cytoplasm of $2A^{pro}$-expressing cells in a dose-dependent manner but accumulated in the nuclear fraction (Fig. 1E). The C/N ratio of rRNA 18S was reduced from 6 to 3.2 by the electroporation of 1 or 9 μg of IRES-2A mRNA, respectively (Fig. 1F). The relative level of U2 snRNA was maintained in the cytoplasm but increased in the nucleus (Fig. 1E). Consequently, the C/N ratio of U2 snRNA was also reduced by the PV protease in a dose-dependent manner (Fig. 1F). By contrast, distribution of tRNA-Val in cytoplasmic and nuclear fractions was not affected by $2A^{pro}$ (Fig. 1E,F). Therefore, $2A^{pro}$ blocks rRNA and U snRNA transport from the nucleus to the cytoplasm, whereas the pathway used by tRNA export remains functional.

To analyze the contribution of the half-life of β-actin mRNA to the insensitivity to $2A^{pro}$, we added actinomycin D, a potent inhibitor of cellular transcription, to HeLa X1/5 culture cells and analyzed protein synthesis at 4 and 8 hpe. Transcription was halted by this compound because luciferase activity was dramatically reduced in treated cells (supplementary material Fig. S2A). By contrast, treatment with actinomycin D weakly inhibited β-actin synthesis, suggesting that β-actin mRNA is very stable in HeLa cells (supplementary material Fig. S2B).

### PV $2A^{pro}$ hampers nuclear export of cellular polyadenylated mRNAs

Next, we decided to assay the impact of PV $2A^{pro}$ on the export of bulk cellular mRNAs using in-situ-hybridization assays with a fluorescein-labeled oligo d(T) probe against poly(A) tail. Oligo d(A) probe or a mixture of both probes [either 1:1 or 5:1 ratio of oligo d(A) to oligo d(T)] was used as a control (supplementary material Fig. S3A). Nuclei and cytoplasm were stained by indirect immunofluorescence using antibodies raised against Ref-1/Aly and α-tubulin. Fluorescent oligo d(T) localized in the nucleus and cytoplasm of HeLa cells, whereas no fluorescent signal was detected from the oligo d(A) probe (supplementary material Fig. S3A). As expected, abrogation of oligo d(T) staining occurred when oligo d(A) was added to the hybridization mixture in a dose-dependent manner, suggesting that exogenous oligo d(A) competes with poly(A) tail by binding to oligo d(T) (supplementary material Fig. S3A). Therefore, we can conclude that our hybridization assays with oligo d(T) specifically detect polyadenylated mRNAs.

Next, in situ hybridization with oligo d(T) probe was carried out at 16, 24 and 48 hpe in control cells or cells expressing IRES-2A. In control cells, poly(A)-containing mRNAs localized to brightly staining foci in the nucleus, which were excluded from nuclear structures consistent with nucleoli (Fig. 2A,B). Conversely, a diffuse distribution of mRNAs was observed in the cytoplasm (Fig. 2A,B). Nuclear fluorescence increased slightly in cells electroporated with 1 μg IRES-2A mRNA but no significant differences were observed in the intensity and the distribution of hybridized oligo d(T) in the cytoplasm (Fig. 2A). These data indicate that $2A^{pro}$ synthesized in low quantities has a moderate effect on mRNA export. However, cells electroporated with 9 μg IRES-2A mRNA exhibited notable differences in the fluorescence pattern.

The evolution of these alterations could progress as follows: (i) dissolution of nuclear foci, which is accompanied by increased fluorescence throughout the nucleus excluded from nucleoli (Fig. 2A,B); (ii) generation of mRNA-containing granules in the cytoplasm, possibly corresponding to stress granules (Fig. 2A,B); (iii) reduction of relative levels of cytoplasmic mRNAs (Fig. 2B); and (iv) chromatin condensation, which is apparent at 24-48 hpe when To-Pro-3 is used, suggesting the induction of an apoptosis response (data not shown). Interestingly, expression of an inactive point mutant of PV 2A protease from IRES-2AM2 mRNA (Ventoso et al., 1998) did not affect the distribution of the polyadenylated pool of cellular mRNAs as compared with that in control HeLa cells (supplementary material Fig. S3B). Together, these data indicate that PV $2A^{pro}$ activity abrogates mRNA export from the nucleus. Interestingly, a moderate accumulation of mRNAs in the nuclei of PV $2A^{pro}$-expressing cells was detected at earlier time points (8 hpe), but no effect was observed on mRNA levels in the cytoplasm (supplementary material Fig. S4), which is in agreement with the findings reported for PV infection at early time-points (Park et al., 2008). These data indicate that PV $2A^{pro}$ might block the transport of some induced cellular mRNAs soon after their expression, but that there is a weak effect on the distribution of stable and constitutively synthesized mRNAs over-represented in the cytoplasm, such as β-actin.

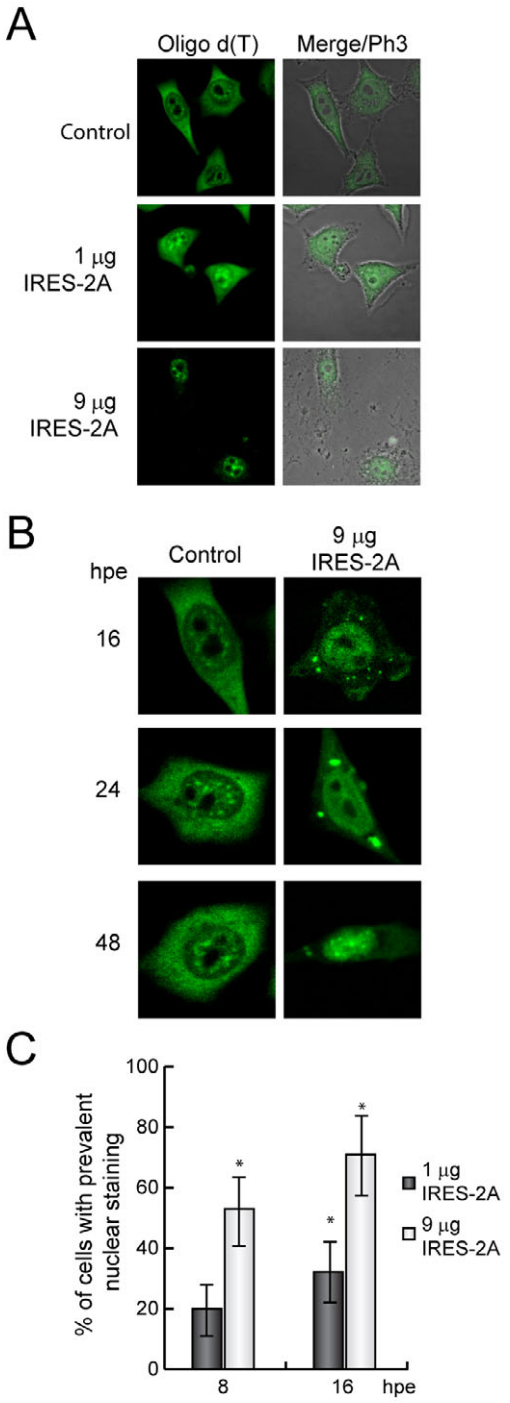


**Fig. 2.** Distribution pattern of polyadenylated mRNAs in HeLa X1/5 cells electroporated with IRES-2A mRNA. HeLa X1/5 cells were electroporated with 1 or 9 μg IRES-2A mRNA or with transcription buffer as control. At 16, 24 and 48 hpe, cells were fixed and in situ hybridization with fluorescein-labeled oligo d(T) probe was carried out. (A) oligo d(T) distribution in control or $2A^{pro}$-expressing cells at 16 hpe. Merge/Ph3 shows the simultaneous visualization of oligo d(T) and the images obtained with phase contrast microscopy. (B) Detail of oligo d(T) distribution in control or $2A^{pro}$-expressing cells at 16, 18 or 24 hpe. (C) Quantitation of cells transfected with 1 (black bars) or 9 μg (white bars) IRES-2A mRNA with an increase in nuclear oligo d(T) staining. Specific fluorescein staining in nucleus and cytoplasm was monitored with MetaMorph software. Represented values are means ± s.d. from three independent experiments. *$P$<0.05, **$P$<0.01, compared with control (not shown), calculated using the Student's $t$-test.

### PV $2A^{pro}$ induces the proteolysis of nucleoporins in HeLa cells

RNAs and proteins are transported between the nucleus and the cytoplasm by signal-mediated and energy-requiring processes that involve many components of the NPC. Nup98, Nup153 and Nup62 have been reported to be cleaved in PV-infected cells (Gustin and Sarnow, 2001; Gustin and Sarnow, 2002; Park et al., 2008). Nup98 is proteolyzed soon after PV infection, whereas Nup153 and Nup62 cleavage need viral replication and, consequently, higher amounts of viral proteins. The proteases that trigger nucleoporin hydrolysis in infected cells are still unknown, although rhinovirus $2A^{pro}$ induces the cleavage of Nup98 in cell-free systems (Park et al., 2008). To examine nucleoporin integrity after $2A^{pro}$ expression, Nup98, Nup153 and Nup62 were analyzed by using western blots of extracts from cells electroporated with IRES-2A mRNA. As expected, 1 μg of IRES-2A mRNA was sufficient to accomplish the complete cleavage of eIF4GI, whereas 9 μg of this mRNA was needed to significantly proteolyze eIF4GII (Fig. 3A). Cleavage of Nup98 was significant with 1 μg IRES-2A mRNA (Fig. 3B), demonstrating that low amounts of PV $2A^{pro}$ are required to induce the proteolysis of this host factor. By contrast, hydrolysis of Nup62 and Nup153 was partially observed in cells electroporated with 9 μg IRES-2A mRNA, and their cleavage was almost total when 30 μg was used (Fig. 3B). These results illustrate that disruption of NPC integrity is dependent on the dose of IRES-2A mRNA employed.

The fact that Nup98 cleavage requires low levels of PV $2A^{pro}$ suggests that Nup98 might be an authentic substrate for this protease. Cleavage of Nup98 results in products of about 55 and 20 KDa in PV-infected cells (Park et al., 2008), but they were not detected using our antibodies (Fig. 3B). It remains possible that these polypeptides might be unstable under the experimental conditions used in this study. The cleavage products derived from Nup153 and Nup62 were also poorly detected by western blot analysis (Fig. 3B). Nup98, Nup153 and Nup62 were not cleaved in cells electroporated with IRES-2AM2 mRNA, which encodes an inactive point mutant of PV $2A^{pro}$, suggesting that protease activity is essential to induce damage in the NPC components (Fig. 3B). Interestingly, components of mRNA nuclear export pathways such as Ref-1/Aly (Fig. 3C), CBP80 and CBP20 (data not shown), as well as other RNA-binding proteins relevant for the control of post-transcriptional events such as polypyrimidine tract-binding protein (data not shown) or splicing factor 45 (spf45) (Fig. 3C), were not proteolyzed when $2A^{pro}$ was expressed from IRES-2A mRNA in HeLa cells. Previously, gemin-3 was described as a specific target for PV $2A^{pro}$ (Almstead and Sarnow, 2007); however, proteolysis of this substrate was not observed in our assays, irrespective of the IRES-2A mRNA dose employed (Fig. 3C). Perhaps, cleavage of gemin-3 requires higher amounts of PV $2A^{pro}$.

To further study Nup98 as a selective substrate of PV $2A^{pro}$, in-vitro-transcribed GST-Nup98 mRNA was translated in HeLa extracts in the presence of [$^{35}$S]Met/Cys for 2 hours. The translation reaction was stopped with cycloheximide and then 1 μg of purified maltose binding protein (MBP), MBP-2A or MBP-3C were added to the reaction mixture and incubated for 1 hour. GST-Nup98 recombinant protein showed a band at about 120 KDa (Fig. 3D). This protein was detected in MBP and MBP-3C-treated extracts but was absent in the presence of MBP-$2A^{pro}$ (Fig. 3D). In fact, two cleavage products with an apparent molecular mass of about 70 and 60 KDa were weakly detected in MBP-2A-treated extracts. Taking into account the molecular mass of GST, the size of 70 KDa for the polypeptide agrees well with the 50 KDa cleavage product described previously in rhinovirus $2A^{pro}$-treated extracts (Park et

al., 2008). Thus, exogenous $2A^{pro}$, but not $3C^{pro}$, triggers the degradation of de-novo-synthesized GST-Nup98 in a cell-free system, suggesting that Nup98 might be an authentic substrate for PV $2A^{pro}$.

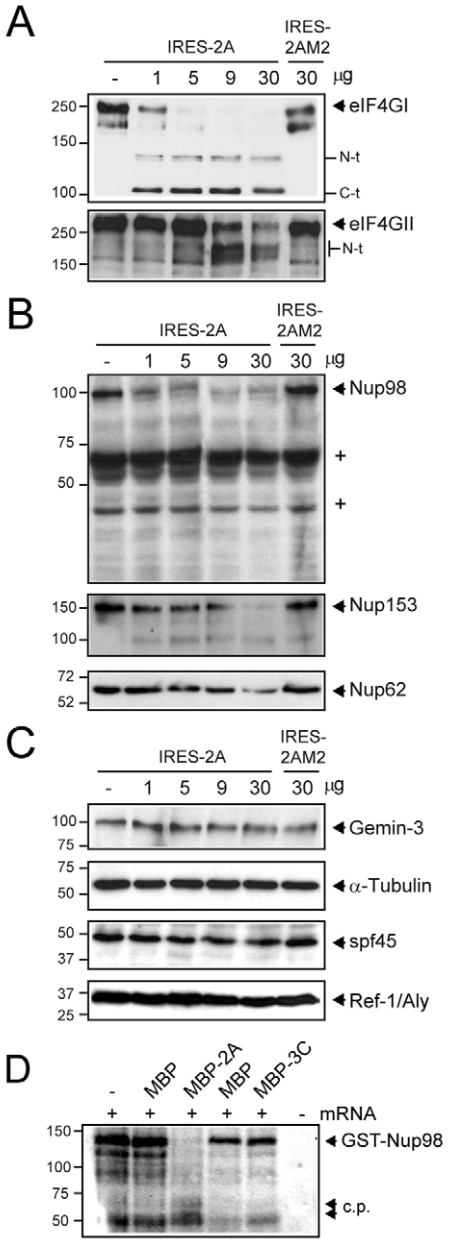


**Fig. 3.** Nucleoporins are cleaved in PV $2A^{pro}$-expressing HeLa cells. (A) HeLa X1/5 cells were electroporated with 1, 5, 9 or 30 µg IRES-2A mRNA. As controls, 30 µg IRES-2AM2 or transcription buffer were used. At 8 hpe, samples were analyzed by western blotting with antibodies raised against different host proteins as indicated. (A) Western blot against eIF4GI (upper panel) and eIF4GII (lower panel). (B) Integrity of Nup98 (upper panel), Nup153 (middle panel) and Nup62 (lower panel) was determined by western blot. + shows an unspecific polypeptide. (C) In parallel, steady-state levels of gemin-3 (upper panel), α-tubulin (middle upper panel), spf45 (middle lower panel) and Ref-1/Aly (lower panel) were analyzed in extracts from control and $2A^{pro}$-expressing cells. (D) Nuclease-treated HeLa extracts were programmed with 200 ng of GST-Nup98 mRNA in the presence of [$^{35}$S]Met-[$^{35}$S]Cys for 2 hours at 30°C. Cycloheximide was added to the mixtures and then extracts were incubated with 1 µg of MBP, MBP-2A or MBP-3C. Reactions were stopped after 1 hour and the radiolabeled polypeptides detected by SDS-PAGE followed by fluorography and autoradiography.

Next, the subcellular distribution of Nup98 or Nup214, Nup153 and Nup62 (QE3 monoclonal antibody) was analyzed by indirect immunofluorescence. In control cells, all these nucleoporins were localized at the nuclear rim, as expected for NPC components, although a smaller bulk of nucleoporins was also detected in the cytoplasm and nucleoplasm (Fig. 4). Electroporation with 1 µg IRES-2A mRNA induced slight disruptions in the distribution of nucleoporins at the nuclear rim, especially in the case of Nup98 (Fig. 4, see detail). In addition, nucleoporin-containing nucleoplasmic granules were not detected in these cells, suggesting that movement of nucleoporins throughout the nucleoplasm could be inhibited (Fig. 4, see detail). Conversely, the electroporation of 9 µg IRES-2A mRNA induced substantial alterations in nucleoporin distribution. Nup98 disappeared from the nuclear envelope and appeared in the perinuclear region or in cytoplasmic granules or spots (Fig. 4, see detail). Subsequently, nucleoporin staining at the nuclear rim was irregular, with areas lacking these NPC components. These alterations were not detected when PV $2A^{pro}$ M2 was expressed in HeLa cells, indicating that protease activity is essential for the redistribution of nucleoporins achieved in wild-type PV $2A^{pro}$-expressing cells (Fig. 4). Ref-1 (Fig. 4) as well as other nuclear proteins such as PARP or p53 and DNA (data not shown) remained in the nucleus of HeLa cells expressing $2A^{pro}$, indicating that the selective barrier that conforms the nuclear envelope and NPC is not disrupted, despite nucleoporin cleavage.

### Expression of FMDV $L^{pro}$ or PV $3C^{pro}$ in HeLa cells does not affect the integrity of nucleoporins and the trafficking of nuclear mRNAs

To determine whether other picornavirus proteases induce the cleavage of nucleoporins, HeLa cells were electroporated with mRNAs encoding foot and mouth disease virus (FMDV) $L^{pro}$ or PV $3C^{pro}$. Electroporated cells were recovered at 8 hpe, and protein synthesis and potential cleavage of initiation factors and nucleoporins were examined. Expression of both PV $2A^{pro}$ and FMDV $L^{pro}$ led to the shut-off of protein synthesis in a dose-dependent manner (Fig. 5A). Consistent with previous observations (Castello et al., 2006a), inhibition of cellular translation correlated with the proteolysis of eIF4GI and eIF4GII (Fig. 5A,B). Interestingly, expression of PV $3C^{pro}$ from cells electroporated with IRES-3C mRNA did not inhibit protein synthesis, and eIF4GI and eIF4GII remained largely intact (Fig. 5A,B). Because the expression of $3C^{pro}$ from pTM1-3C plasmid in COS-7 cells gives rise to an active $3C^{pro}$ (data not shown), we hypothesize that higher amounts of this protease might be required to affect host translational machinery.

In contrast to PV 2A-expressing cells, Nup98 was not proteolyzed in cells electroporated with IRES-L mRNA or IRES-3C mRNA (Fig. 5C). Thus, Nup98 might not be a common substrate for picornaviral proteases, despite the fact that FMDV $L^{pro}$ and PV $2A^{pro}$ share some substrates, such as eIF4GI and eIF4GII (Fig. 5B). Nup153 and Nup62 remained unaltered in cells electroporated with IRES-3C mRNA, but a slight decrease in the steady state level of Nup62 was observed in $L^{pro}$-expressing cells (Fig. 5C). Ref-1/Aly, spf45 or α-tubulin levels were not affected by the expression of these proteases (Fig. 5D).

Although FMDV $L^{pro}$ and PV $3C^{pro}$ did not cleave Nup98 in electroporated cells, it was of interest to assess whether these proteases could affect the distribution of polyadenylated mRNAs. As described in Fig. 2, PV $2A^{pro}$ induced a clear accumulation of mRNAs in the nuclei of HeLa cells, although many of these cells

showed cell rounding that is a typically observed during the long-term expression of viral proteases (Fig. 6). Nuclear staining foci disappeared and polyadenylated mRNAs localized throughout the nucleus. In particular, the C/N ratio of oligo-d(T)-derived fluorescence dropped from ~2 to 1 in most cells. In contrast to PV2A$^{pro}$, electroporation with IRES-L mRNA did not substantially alter the distribution of polyadenylated mRNAs, although the cell rounding was also detected (Fig. 6). Oligo d(T) nuclear staining foci were observed in these cells (Fig. 6), the C/N ratio being approximately 1.7. Finally, the expression of 3C induced a similar oligo d(T) staining pattern to that in control cells (Fig. 6). In fact, the C/N ratio of oligo d(T) fluorescence was similar to that observed in control cells. These data indicated that mRNA traffic seems not to be inhibited in cells electroporated with IRES-L mRNA.

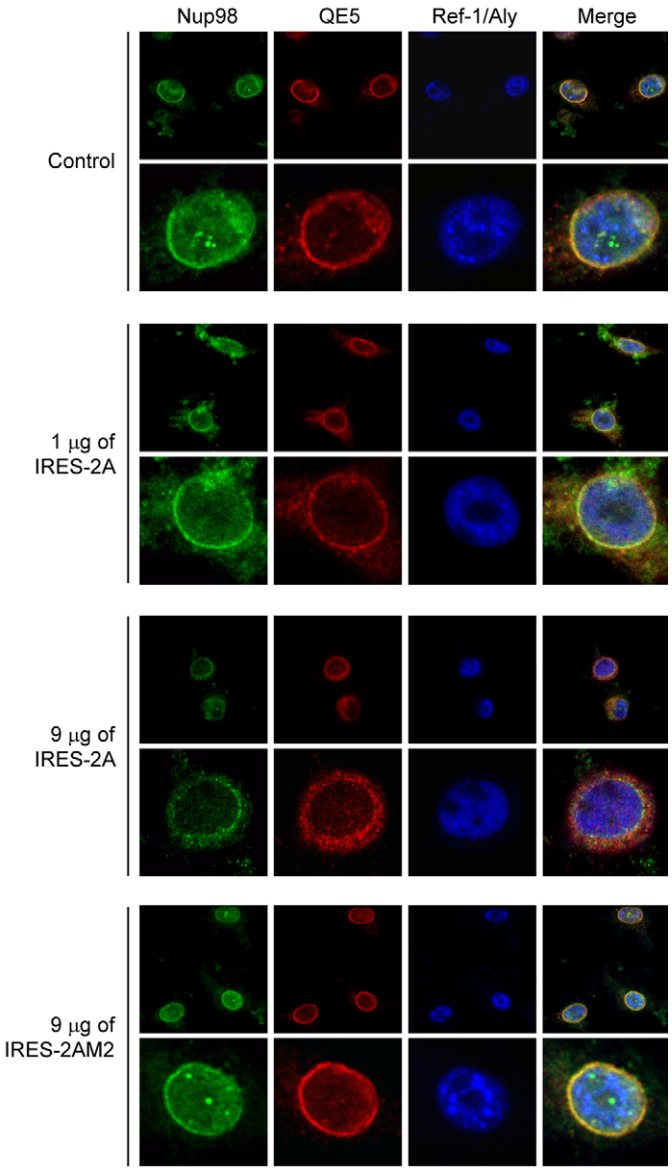


**Fig. 4.** Nucleoporins are redistributed in PV 2A$^{pro}$-expressig cells. HeLa X1/5 cells electroporated with either 1 or 9 μg IRES-2A mRNA, 9 μg of IRES-2AM2 mRNA or with transcription buffer as a control, were seeded after electroporation on coverslips. At 16 hpe, cells were fixed and immunofluorescence was performed using anti-Nup98 (green) and mouse monoclonal antibody QE5 (red). Cells were visualized with a confocal microscope and images were processed with Huygens 3.0 software. Merge shows the simultaneous visualization of Nup98, QE5 antibody and Ref-1/Aly.

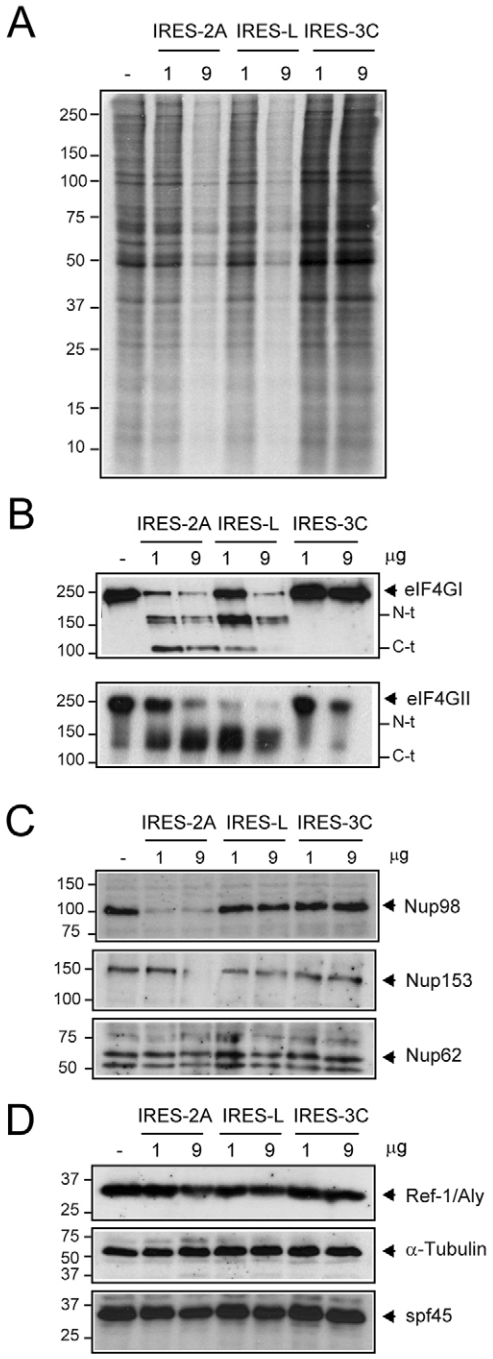


**Fig. 5.** Nup98 remains intact in FMDV L$^{pro}$- or PV 3C$^{pro}$-expressing cells. HeLa X1/5 cells were electroporated with either 1 or 9 μg of IRES-2A, IRES-L or IRES-3C mRNAs or with transcription buffer as a control. From 7 to 8 hpe, protein synthesis was labeled with [$^{35}$S]Met/Cys. At 8 hpe, protein synthesis and the integrity of host factors were analyzed. (A) Total proteins were separated by SDS-PAGE and then fluorography and autoradiography was carried out. (B) Western blot analysis against eIF4GI (upper panel) and eIF4GII (lower panel). (C) Integrity of Nup98 (upper panel), Nup153 (middle panel) and Nup62 (lower panel) was determined by western blot. (D) In parallel, levels of Ref-1/Aly (upper panel), α-tubulin (middle panel) and spf45 (lower panel) were analyzed.

### Effect of IFN-γ on RNA nuclear export in 2A$^{pro}$-expressing cells

Interferon (IFN)-γ induces the expression of a wide variety of genes, many of which are involved in the antiviral response (Levy and Garcia-Sastre, 2001). In particular, the relative level of Nup98 increases with IFN-γ treatment and, under such conditions, vesicular stomatitis virus (VSV) M protein is not able to inhibit RNA nuclear export (Enninga et al., 2002). Thus, we looked at whether IFN-γ prevents the blockage of RNA trafficking induced by PV 2A$^{pro}$. The amount of Nup98 was enhanced approximately threefold after the treatment of HeLa X1/5 cells for 16 hours with 250 U of IFN-γ (supplementary material Fig. S5A), whereas the steady-state levels of eIF4GI, Nup62, Ref-1/Aly or eIF4E were not affected (supplementary material Fig. S5A). As shown in Fig. 7A, Nup98 was proteolyzed in untreated 2A$^{pro}$-expressing cells, whereas Nup214, Nup153 and Nup62 were only slightly affected. Notably, the expression of 2A$^{pro}$ in IFN-γ treated cells induced only a slight decrease (of ~30%) in Nup98 levels (Fig. 7A).

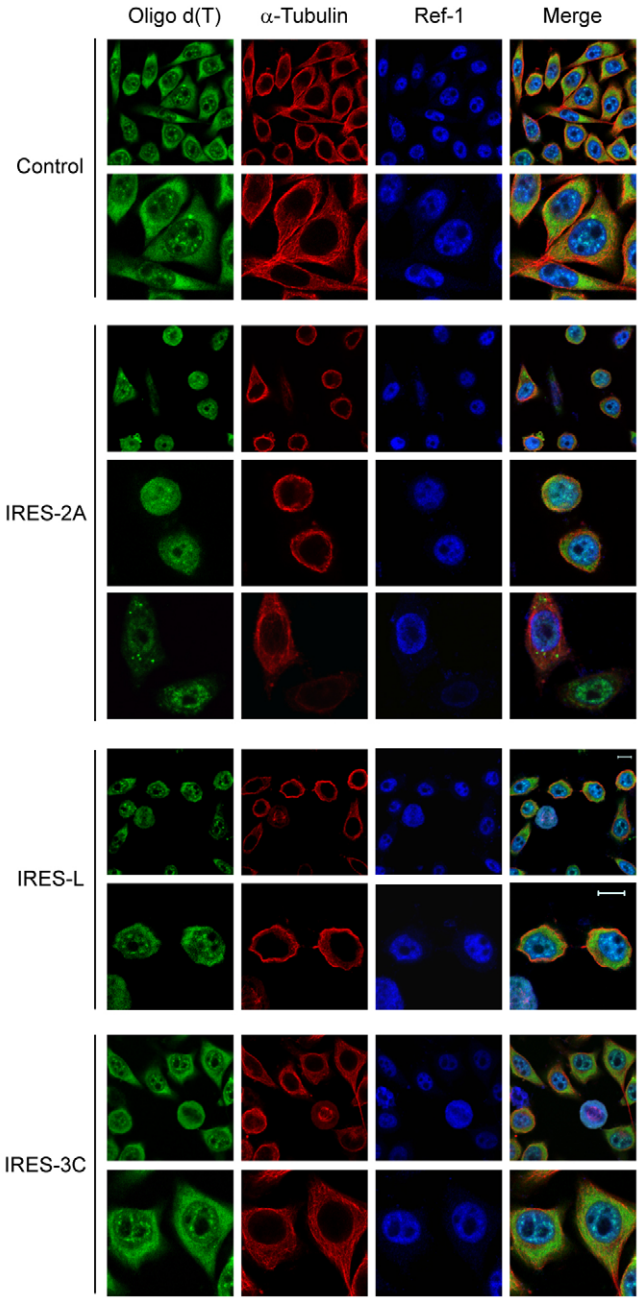


**Fig. 6.** Impact of the expression of PV 2A$^{pro}$, 3C$^{pro}$ and FMDV L$^{pro}$ on export of polyadenylated mRNAs. HeLa X1/5 cells were electroporated with 9 µg IRES-2A, IRES-L or IRES-3C mRNAs or with transcription buffer as a control. At 16 hpe, cells were fixed and in situ hybridization with fluorescein-labeled oligo d(T) probe was carried out to detect polyadenylated mRNAs. Anti-Ref-1/Aly antibody was used as a nuclear marker, and α-tubulin antibody was used as a cytoplasmic marker. All samples were visualized with a confocal microscope. Merge shows the simultaneous visualization of oligo d(T), α-tubulin and Ref-1/Aly. Scale bars: 10 µm.

To determine the subcellular localization of Nup98 in 2A$^{pro}$-expressing and IFN-γ-pretreated cells, indirect immunofluorescence was carried out. Nup98 was weakly detected at the nuclear rim in untreated cells, followed by the appearance of cytoplasmic accumulations (Fig. 7B). However, a significant amount of Nup98 was detected at the nuclear envelope in IFN-γ-treated cells when 2A$^{pro}$ was expressed (Fig. 7B), indicating that a pool of this nucleoporin remained unaltered under these conditions. The subcellular distribution of 18S rRNA, tRNA-Val, U2 snRNA and β-actin, COX-2, c-myc and IL-6 mRNAs in nuclear and cytoplasmic fractions was then examined by real-time RT-PCR (Fig. 7C) and the purity of the fractions determined by western blot (supplementary material Fig. S5A). As shown previously, the amount of IL-6 and c-myc mRNAs as well as U2 snRNA significantly increased with 2A$^{pro}$-expression (Fig. 7C). In contrast to the data obtained from untreated cells (Fig. 1), mRNAs from cells pretreated with IFN-γ exhibited the same C/N ratio in control and 2A$^{pro}$-expressing cells (Fig. 7D). These results indicate that IFN-γ prevents the inhibition of RNA nuclear export induced by PV 2A$^{pro}$.

To examine the possibility that IFN-γ inhibited 2A$^{pro}$ expression in treated cells, the cleavage of eIF4GI and eIF4GII were examined in extracts from treated and untreated cells. Fig. 7E shows that both eIF4GI and eIF4GII were also proteolyzed with 2A$^{pro}$ expression, in spite of IFN-γ treatment. In addition, translation of an EMCV IRES containing luciferase reporter mRNA (IRES-Luc) (Castello et al., 2006a) was only slightly affected by IFN-γ treatment (Fig. 7F). Taken together, these observations suggest that IFN-γ did not affect substantially EMCV IRES-driven translation.

## Discussion

Virus infection usually induces host responses aimed at interfering with viral replication. For that reason, viruses have developed diverse strategies to evade or attenuate the antiviral epigenetic defence program of cells. PV targets host gene expression at different stages, including transcription, nuclear import and export of proteins, and translation (Gustin and Sarnow, 2001; Gustin and Sarnow, 2002; Lloyd, 2006; Weidman et al., 2003). Several transcription factors are activated in virus-infected cells and are imported to the nucleus to trigger the transcription of genes with antiviral activity (Randall and Goodbourn, 2008). Thus, inhibition of nuclear import of proteins by PV could block the activation of host gene responses. Our present findings indicate that PV 2A$^{pro}$ could also impair RNA export from the nucleus to the cytoplasm.

This phenomenon requires low amounts of PV 2A$^{pro}$ and, subsequently, appears to occur before the impairment exerted by this protease on cellular transcription and translation. Inhibition of both protein import and RNA export might work to ensure the progression of viral infection and to impair the establishment of a hostile cellular environment. In fact, several mRNAs are induced by 2A$^{pro}$ expression, including the immunomodulator IL-6 and regulators of cell proliferation, survival and death such as p53 and

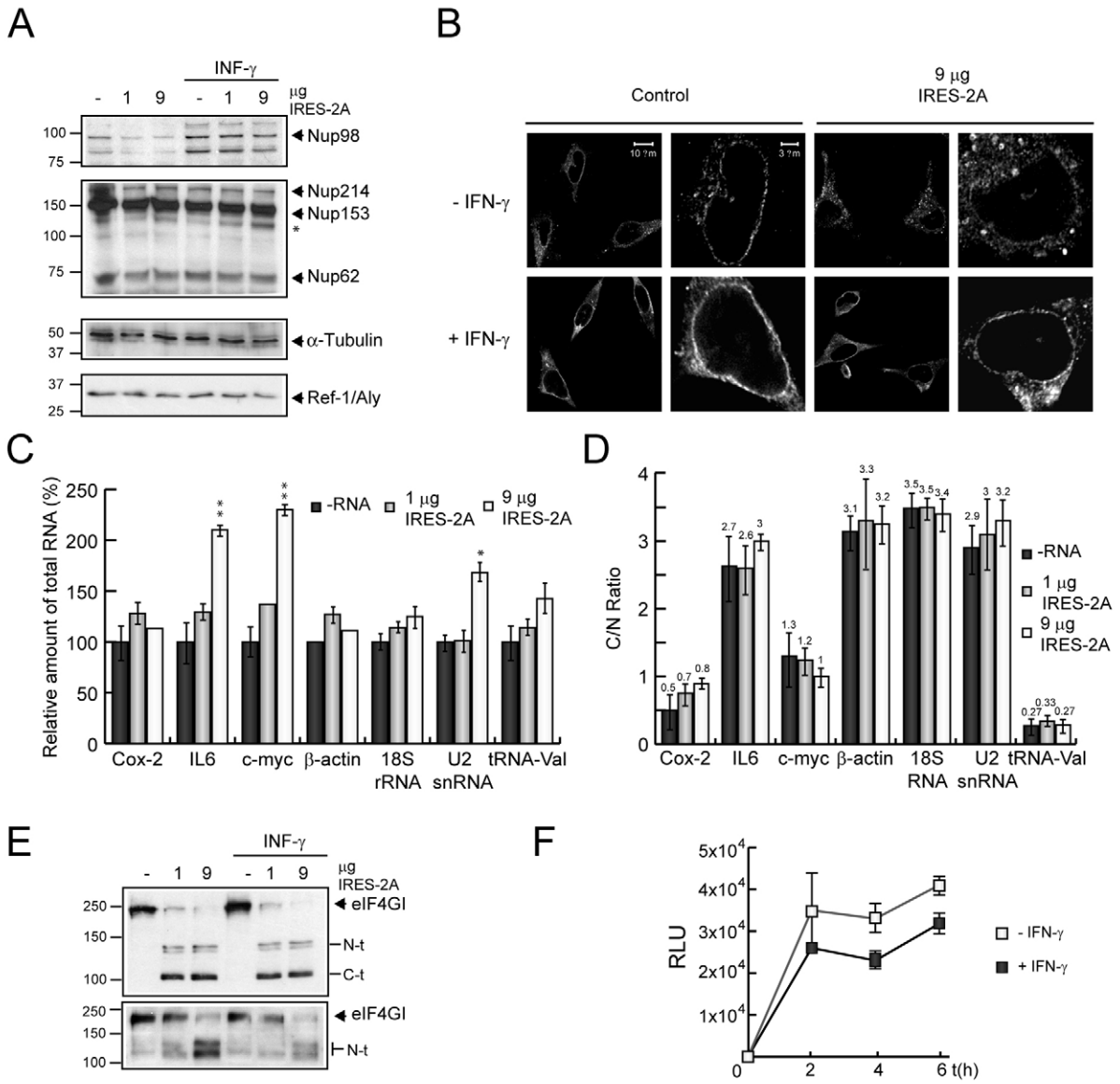


**Fig. 7.** IFN-γ pretreatment rescues the blockade of RNA nuclear export in HeLa cells that express PV $2A^{pro}$. HeLa X1/5 cells were pre-incubated with 250 U Hu-IFN-γ for 24 hours. Hu-IFN-γ pretreated or mock cells were then electroporated with either 1 or 9 μg IRES-2A mRNA or with transcription buffer as a control. (A) At 8 hpe, post-electroporated cells were recovered in sample buffer, and western blotting with antibodies raised against Nup98 (upper panel), Nup153, Nup62, Nup214 (middle upper panel), α-tubulin (middle bottom panel) and Ref-1/Aly (bottom panel) were carried out. * indicates a putative cleavage product. (B) Electroporated cells, treated as described above, were seeded on coverslips and fixed at 8 hpe. Immunofluorescence analysis was performed with anti-Nup98 antibody. Cells were visualized with a confocal microscope and images processed with Huygens 3.0 software. (C,D) HeLa X1/5 cells, pre-incubated with 250 U IFN-γ for 16 hours were electroporated with either 1 or 9 μg of IRES-2A mRNA, or with transcription buffer as a control. Total, nuclear and cytoplasmic fractions were isolated in each case at 8 hpe. COX-2, IL-6, c-myc, and β-actin mRNAs and 18S rRNA, U2 snRNA and tRNA-val were quantified in each fraction by real-time RT-PCR using specific oligonucleotides and Taqman probes. (C) The represented values show the relative levels of each mRNA in the total fraction from control (black bars) and cells electroporated with 1 (grey bars) or 9 (white bars) IRES-2A mRNA. (D) C/N ratio was calculated for each RNA from control (black bars) or 2A-expressing cells (grey and white bars). (E) Proteolytic activity of PV $2A^{pro}$ in IFN-γ treated or untreated cells was analyzed by western blotting against its substrates eIF4GI and eIF4GII. (F) HeLa cells were treated in parallel for 16 hours with or without IFN-γ and then electroporated with 9 μg of IRES-Luc. Luciferase activity from IFN-γ treated (black squares) and untreated extracts (white squares) was determined at 2, 4 and 6 hpe. RLU, relative light units. Values are means ± s.d. $*P<0.05$, $**P<0.01$, compared with control, calculated using the Student's *t*-test.

c-myc. However, these mRNAs did not arrive at the cytoplasm, suggesting that the viral protease can block the cellular gene response in this manner. In fact, apoptosis is triggered at later times post-electroporation (24-48 hpe), despite the early increase in p53 mRNA levels in $2A^{pro}$-expressing cells. In addition, de-novo-synthesized luciferase mRNAs accumulate dramatically in the nucleus but disappear from cytoplasmic fractions in cells electroporated with IRES-2A mRNA. Conversely, distribution of constitutively synthesized mRNAs such as β-actin is not significantly altered by $2A^{pro}$ at 8 hpe. Therefore, blockade of RNA traffic might not be the cause of the global protein synthesis shut-off observed in $2A^{pro}$-expressing or PV-infected cells.

PV $2A^{pro}$ not only interferes with the nuclear export of mRNAs but also with the traffic of rRNAs and U snRNAs. However, export

of tRNAs from the nucleus is not affected by the PV protease. A similar result was observed for vesicular stomatitis virus (VSV) M protein, suggesting a common target for both viral proteins (Her et al., 1997; Petersen et al., 2000). Nevertheless, the possible role of the inhibition of rRNA and U snRNA trafficking in PV infection needs further investigation. We can speculate that both the protein synthesizing machinery and/or the splicing activity might also be affected.

Exchange of macromolecules between the nucleus and cytoplasm takes place exclusively through the NPC. In fact, each NPC is able to orchestrate hundreds of transport events per minute (Ball and Ullman, 2005). This abundant selective traffic makes the NPC a key target during viral infections because the virus aims to block the transport of RNAs and proteins between these two subcellular compartments. $2A^{pro}$ targets the NPC directly or indirectly by cleaving different nucleoporins such as Nup153, Nup62 and specially Nup98. Immunofluorescence assays revealed that the amount of the three nucleoporins recognized by QE5 antibody (Nup153, Nup62 and Nup214) diminished in $2A^{pro}$-expressing cells, whereas Nup98 disappeared from the nuclear rim and was relocalized in the cytoplasm. These nucleoporins are essential components of the NPC and mediate import and export of proteins and RNAs through the NPC by means of interactions with crucial components of the different traffic pathways (Galy et al., 2003; Harborth et al., 2001). For example, Nup153 binds importin-5/Kapβ3/RanBP5, importin-7/RanBP7, exportin-5, exportin-t, exportin-1, NXF1/Tap (the export receptor of mRNAs), Impα2 and NTF2 (the import receptor of Ran) (Ball and Ullman, 2005). Furthermore, Nup98 interacts with Rae-1, an adaptor for NXF1/Tap-dependent export (Pritchard et al., 1999).

Interaction domains in nucleoporins are related to an unfolded subset of glycosylated FG (phenylalanine-glycine) repeats located at the C-terminal portion of the protein. The relevance of this domain in RNA export was demonstrated using specific antibodies (Featherstone et al., 1988; Neuman de Vegvar and Dahlberg, 1990; Terns and Dahlberg, 1994). Therefore, alteration of the NPC by PV $2A^{pro}$ might uncouple export and import machinery from the NPC. In this regard, VSV M protein also targets the NPC. This viral protein interacts with Rae-1/mrnp41 and with Nup98 at the FG domain, inhibiting cellular RNA export (Faria et al., 2005; von Kobbe et al., 2000). In addition, influenza virus NS1 protein forms an inhibitory complex with NXF1/TAP, p15/NXT, Rae-1/mrnp41 and E1B-AP5 and downregulates Nup98 (Satterly et al., 2007). Analogies between VSV M, influenza virus, NS1 and PV $2A^{pro}$ could point to the NPC as an important target for several nuclear and cytoplasmic viruses.

Nup98 and Nup153 are mobile components of the NPC and their dynamics are dependent on active transcription, suggesting a link between RNA cargo formation and the status of ongoing pore reconfiguration. In particular, mobility of Nup98 and Nup153 are related to RNA polymerase (Pol) I and II activity (Griffis et al., 2002; Griffis et al., 2004). Given that Pol I transcribes long rRNAs, Pol II synthesizes U snRNAs and mRNAs, and Pol III generates tRNAs, Nup98 and Nup153 might be involved in export of rRNAs, U snRNAs and mRNAs but not of tRNAs (Kohler and Hurt, 2007). For that reason, tRNAs might be insensitive to the cleavage of nucleoporins (Fig. 1D-F). Alternatively, exportin-t, the transporter involved in tRNA export (Cullen, 2003; Kohler and Hurt, 2007), could work despite damage to the NPC induced by PV $2A^{pro}$ or VSV M. Cleavage of nucleoporins Nup153, Nup62 and Nup98 was previously observed in PV and rhinovirus-infected cells (Gustin and Sarnow, 2001; Gustin and Sarnow, 2002; Park et al., 2008). However, the protease(s) involved in NPC damage is still unknown.

Interestingly, alterations in the NPC induced in vitro by PV are blocked with PV $2A^{pro}$ inhibitors such as elastatinal, elastase and MPCMK (Belov et al., 2004). These data strongly suggest that PV $2A^{pro}$ is directly or indirectly responsible for nucleoporin cleavage. Caspase-3 and/or caspase-9 can also hydrolyze Nup153, rendering a cleavage product similar to that observed in PV $2A^{pro}$-expressing cells. However, Nup62 is not proteolyzed by caspases in HeLa cells after induction of apoptosis (Buendia et al., 1999). Moreover, PV infection also alters the NPC in cells lacking active caspase-3 and caspase-9 (Belov et al., 2004). These results indicate that these apoptosis executors are not involved in the proteolysis of nucleoporins in PV-infected cells. Our data indicate that expression of PV $2A^{pro}$ alone is sufficient to induce nucleoporin cleavage in transfected HeLa cells or in cell-free systems. By contrast, expression of an inactive mutant of PV $2A^{pro}$ did not affect the integrity of nucleoporins. In addition, electroporation of IRES-3C mRNA (which encodes $3C^{pro}$, the other protease of PV) did not induce the proteolysis of nucleoporins nor the inhibition of mRNA traffic. Taking these results together, we hypothesize that PV $2A^{pro}$ is the protease involved in directly or indirectly targeting the NPC during PV infection. Interestingly, other related proteases, such as FMDV $L^{pro}$, share with PV $2A^{pro}$ some substrates such as eIF4GI and eIF4GII but both proteases differ in their ability to cleave Nup98. Thus, low doses of PV $2A^{pro}$ (1 μg IRES-2A mRNA) give rise to the cleavage of Nup98, whereas this protein remains unaltered after FMDV $L^{pro}$ expression. Consequently, FMDV $L^{pro}$ did not affect substantially the distribution of the pool of polyadenylated mRNAs. Curiously, L protein from EMCV induces the phosphorylation of nucleoporins, leading to the inactivation of nucleus-cytoplasm traffic of macromolecules (Porter et al., 2006; Porter and Palmenberg, 2009). However, we could not observe these effects after expression of FMDV $L^{pro}$.

IFN-γ triggers a host response against viral infection (Randall and Goodbourn, 2008). Strikingly, two components of the RNA nuclear export machinery, Nup98 and Rae-1, are overexpressed in cells treated with IFN-γ (Enninga et al., 2002; Faria et al., 2005). These data suggest that RNA and protein trafficking through the NPC is a key target for successful infection of cytopathic viruses. In fact, inhibition of nuclear RNA export by VSV M is avoided after treatment with IFN-γ, perhaps due to the overproduction of Nup98 and Rae-1 (Enninga et al., 2002; Faria et al., 2005). In addition, we have also observed a specific increase in the Nup98 steady-state level in HeLa cells pre-incubated with 250 U IFN-γ. Under these experimental conditions, Nup98 was partially proteolyzed in $2A^{pro}$-expressing cells and a substantial pool remained at the nuclear membrane. Nevertheless, the amount of Nup153 is not increased when HeLa cells are treated with IFN-γ. These data point to the idea that Nup98 might be an essential component of the nucleus-cytoplasm traffic machinery. The ineffective cleavage of Nup98 in IFN-γ-treated cells is consistent with the restoration of nuclear-cytoplasmic RNA trafficking. Collectively, these findings suggest that IFN-γ is an important host factor in preventing alterations in cellular gene expression induced by viral infections. Therefore, secretion of IFN-γ from immune cells might induce an effective gene response against virus infection in competent neighbouring cells. Future efforts will focus on determining whether cellular components involved in the RNA export machinery are also targeted by other proteins from other cytopathic viruses.

## Materials and Methods

### Cell cultures

Hela X1/5 cells were previously described (Novoa and Carrasco, 1999). Hu-IFN-γ was generously provided by Ali Alejo and Antonio Alcamí (Centro de Biología Molecular 'Severo Ochoa', Madrid, Spain).

### Plasmids, in vitro transcription and RNA transfection

The plasmids pTM1-2A, pTM1-2AM2, pTM1-3C and pTM1-L were used as templates to synthesize in vitro IRES-2A, IRES-2AM2, IRES-3C and IRES-L mRNAs, respectively. The in vitro transcription reaction and transfection of resulting mRNAs were carried out as described previously (Castello et al., 2006a). pGEX-4T-Nup98 CBP20 (a generous gift from Elisa Izaurralde, Max Planck Institute for Developmental Biology, Tübingen, Germany) was previously described (von Kobbe et al., 2000).

### Protein synthesis, subcellular fractionation, western blot and luciferase activity analyses

Determination of protein synthesis was performed by metabolic labeling with 50 μCi of [$^{35}$S]Met-[$^{35}$S]Cys/ml (Promix; Amersham Biosciences) for 1 hour, followed by SDS-PAGE, fluorography and autoradiography. Subcellular fractions were obtained using a buffer containing NP-40, RNaseOUT (Invitrogen) and a cocktail of protease inhibitors (Sigma-Aldrich) as described previously (Perales et al., 2003). eIF4GI was detected with antisera raised against peptides derived from the N-terminal and C-terminal, at 1:1000 dilution (Aldabe et al., 1995). Rabbit antisera against N-terminal and C-terminal region of eIF4GII (a generous gift from Nahum Sonenberg, McGill University, Montreal, Canada) were employed at 1:500 dilution. Mouse antibody against PARP (BD Pharmigen) was used at 1:250 dilution. Mouse antibodies against PABP, gemin-3 (Abcam), PTB, α-tubulin (Sigma) were used at 1:200, 1:1000, 1:1000, and 1:5000 dilutions, respectively. Rabbit antisera against Ref-1/Aly, CBP80, CBP20 (a generous gift from Elisa Izaurralde, Max Planck Institute for Developmental Biology, Tübingen, Germany) and spf45 (a generous gift from Juan Valcárcel, Centre for Genomic Regulation, Barcelona, Spain) were used at 1:1000 dilution. Mouse monoclonal antibody [QE5] (Abcam) was used at 1:1000 dilution for western blot analysis and 1:50 for immunofluorescence. Nup98 was detected in immunofluorescence with rat monoclonal antibody at 1:100 dilution (a generous gift from Maureen A. Powers, Emory University School of Medicine, Atlanta, GA), and with rabbit antisera (Abcam) for western blot analysis at 1:500 dilution. Anti-rabbit (Amersham) and anti-mouse (Promega) immunoglobulin G antibodies coupled to peroxidase were used at 1:5000 dilution. The percentage of protein synthesis and the percentage of intact proteins were determined by densitometric scanning. Measurement of luciferase activity was determined with the Luciferase Assay System kit (Promega) with a Monolight 2010 apparatus (Analytical Luminescence Laboratory, San Diego, CA).

### In vitro translation

The HeLa S3 extracts and the translation reaction mix were obtained as previously described (Franco et al., 2005) and was kindly provided by David Franco (Aaron Diamond AIDS Research Center, The Rockefeller University, New York, NY). GST-Nup98 cleavage was analyzed by metabolic labeling with 50 μCi of [$^{35}$S]Met-[$^{35}$S]Cys/ml (Promix; Amersham Biosciences), followed by SDS-PAGE, fluorography and autoradiography.

### Purification of recombinant proteins

The chimeric MBP (maltose-binding protein), MBP-2A$^{pro}$ and MBP-3C$^{pro}$ were purified by affinity chromatography, as described previously (Novoa and Carrasco, 1999).

### Real-time RT-PCR analyses

Total RNA was isolated from the different fractions using the kit RNAspin mini (GE Healthcare). Analysis of β-actin, luciferase, U2 snRNA and 18S rRNA levels was performed as described previously (Castello et al., 2006a). IL-6, COX-1, COX-2, c-myc and p53 mRNAs were quantified as described previously using primers and probes designed by Applied Biosystems (a generous gift from Manuel Fresno, Centro de Biología Molecular 'Severo Ochoa', Madrid, Spain). Real-time RT-PCR with oligonucleotides designed against tRNA-Val (Roche) was carried out using Master SYBR Green I Kit (Roche) (Castello et al., 2006b). Data analysis was carried out using the SDS-7000 software (Version 1.1).

### Immunofluorescence microscopy and FISH assay

Fixation, permeabilization and confocal microscopy were performed as described previously (Madan et al., 2008), employing a confocal LSM510 lens coupled to an Axiovert 200 M microscope (Zeiss). Image processing was performed with Huygens 3.0 software. Detection of polyadenylated mRNAs by fluorescence in situ hybridization (FISH) was carried out using fluorescein-labeled oligo d(T) or oligo d(A) probes (Gene link). Cells were fixed and permeabilized and then washed three times: first with 1× phosphate-buffered saline (PBS), then with 1× PBS and 1× saline-sodium citrate buffer (SSC), and finally with 2× SSC. Next, cells were incubated at 37°C with pre-hybridation buffer (2× SSC, 20% deionized formamide, 0.2% BSA and 1 mg/ml yeast tRNA). Afterwards, cells were incubated at 37°C for 4 hours with hybridization buffer (2× SSC, 20% deionized formamide, 0.2% BSA, 1 mg/ml yeast tRNA, 10% dextran sulphate and 1 pmol/μl oligo d(T) probe). Preparations were washed four times at 42°C for 5 minutes: the first wash was performed with 2× SSC mixed with 20% formamide; the second with 2× SSC; the third with 1× SSC and 1× PBS; and the last with 1× PBS. FISH was carried out using the immunofluorescence protocol described previously (Madan et al., 2008).

This study was supported by a DGICYT Grant (BFU 2006-02182) and an institutional grant awarded to the Centro de Biología Molecular 'Severo Ochoa' by the Fundación Ramón Areces. We thank Antonio Alcamí, Ali Alejo, David Franco, Elisa Izaurralde, Manuel Fresno, Maureen A. Powers, Nahum Sonenberg and Juan Valcárcel for some of the antibodies and reagents used in this study. We are very grateful for the help of Aurelie Rakotondrafara in the preparation of the manuscript.

## References

**Aldabe, R., Feduchi, E., Novoa, I. and Carrasco, L.** (1995). Efficient cleavage of p220 by poliovirus 2Apro expression in mammalian cells: effects on vaccinia virus. *Biochem. Biophys. Res. Commun.* **215**, 928-936.

**Almstead, L. L. and Sarnow, P.** (2007). Inhibition of U snRNP assembly by a virus-encoded proteinase. *Genes Dev.* **21**, 1086-1097.

**Ball, J. R. and Ullman, K. S.** (2005). Versatility at the nuclear pore complex: lessons learned from the nucleoporin Nup153. *Chromosoma* **114**, 319-330.

**Belov, G. A., Lidsky, P. V., Mikitas, O. V., Egger, D., Lukyanov, K. A., Bienz, K. and Agol, V. I.** (2004). Bidirectional increase in permeability of nuclear envelope upon poliovirus infection and accompanying alterations of nuclear pores. *J. Virol.* **78**, 10166-10177.

**Buendia, B., Santa-Maria, A. and Courvalin, J. C.** (1999). Caspase-dependent proteolysis of integral and peripheral proteins of nuclear membranes and nuclear pore complex proteins during apoptosis. *J. Cell Sci.* **112**, 1743-1753.

**Castello, A., Alvarez, E. and Carrasco, L.** (2006a). Differential cleavage of eIF4GI and eIF4GII in mammalian cells. Effects on translation. *J. Biol. Chem.* **281**, 33206-33216.

**Castello, A., Sanz, M. A., Molina, S. and Carrasco, L.** (2006b). Translation of Sindbis virus 26S mRNA does not require intact eukariotic initiation factor 4G. *J. Mol. Biol.* **355**, 942-956.

**Cullen, B. R.** (2003). Nuclear RNA export. *J. Cell Sci.* **116**, 587-597.

**Enninga, J., Levy, D. E., Blobel, G. and Fontoura, B. M.** (2002). Role of nucleoporin induction in releasing an mRNA nuclear export block. *Science* **295**, 1523-1525.

**Faria, P. A., Chakraborty, P., Levay, A., Barber, G. N., Ezelle, H. J., Enninga, J., Arana, C., van Deursen, J. and Fontoura, B. M.** (2005). VSV disrupts the Rae1/mrnp41 mRNA nuclear export pathway. *Mol. Cell* **17**, 93-102.

**Featherstone, C., Darby, M. K. and Gerace, L.** (1988). A monoclonal antibody against the nuclear pore complex inhibits nucleocytoplasmic transport of protein and RNA in vivo. *J. Cell Biol.* **107**, 1289-1297.

**Franco, D., Pathak, H. B., Cameron, C. E., Rombaut, B., Wimmer, E. and Paul, A. V.** (2005). Stimulation of poliovirus RNA synthesis and virus maturation in a HeLa cell-free in vitro translation-RNA replication system by viral protein 3CDpro. *Virol. J.* **2**, 86.

**Galy, V., Mattaj, I. W. and Askjaer, P.** (2003). Caenorhabditis elegans nucleoporins Nup93 and Nup205 determine the limit of nuclear pore complex size exclusion in vivo. *Mol. Biol. Cell* **14**, 5104-5415.

**Griffis, E. R., Altan, N., Lippincott-Schwartz, J. and Powers, M. A.** (2002). Nup98 is a mobile nucleoporin with transcription-dependent dynamics. *Mol. Biol. Cell* **13**, 1282-1297.

**Griffis, E. R., Craige, B., Dimaano, C., Ullman, K. S. and Powers, M. A.** (2004). Distinct functional domains within nucleoporins Nup153 and Nup98 mediate transcription-dependent mobility. *Mol. Biol. Cell* **15**, 1991-2002.

**Gustin, K. E. and Sarnow, P.** (2001). Effects of poliovirus infection on nucleo-cytoplasmic trafficking and nuclear pore complex composition. *EMBO J.* **20**, 240-249.

**Gustin, K. E. and Sarnow, P.** (2002). Inhibition of nuclear import and alteration of nuclear pore complex composition by rhinovirus. *J. Virol.* **76**, 8787-8796.

**Harborth, J., Elbashir, S. M., Bechert, K., Tuschl, T. and Weber, K.** (2001). Identification of essential genes in cultured mammalian cells using small interfering RNAs. *J. Cell Sci.* **114**, 4557-4565.

**Her, L. S., Lund, E. and Dahlberg, J. E.** (1997). Inhibition of Ran guanosine triphosphatase-dependent nuclear transport by the matrix protein of vesicular stomatitis virus. *Science* **276**, 1845-1848.

**Kohler, A. and Hurt, E.** (2007). Exporting RNA from the nucleus to the cytoplasm. *Nat. Rev. Mol. Cell Biol.* **8**, 761-773.

**Levy, D. E. and Garcia-Sastre, A.** (2001). The virus battles: IFN induction of the antiviral state and mechanisms of viral evasion. *Cytokine Growth Factor Rev.* **12**, 143-156.

**Lidsky, P. V., Hato, S., Bardina, M. V., Aminev, A. G., Palmenberg, A. C., Sheval, E. V., Polyakov, V. Y., van Kuppeveld, F. J. and Agol, V. I.** (2006). Nucleocytoplasmic traffic disorder induced by cardioviruses. *J. Virol.* **80**, 2705-2717.

**Lloyd, R. E.** (2006). Translational control by viral proteinases. *Virus Res.* **119**, 76-88.

**Madan, V., Castello, A. and Carrasco, L.** (2008). Viroporins from RNA viruses induce caspase-dependent apoptosis. *Cell Microbiol.* **10**, 437-451.

**Martinez-Salas, E. and Fernandez-Miragall, O.** (2004). Picornavirus IRES: structure function relationship. *Curr. Pharm. Des.* **10**, 3757-3767.

**Neuman de Vegvar, H. E. and Dahlberg, J. E.** (1990). Nucleocytoplasmic transport and processing of small nuclear RNA precursors. *Mol. Cell. Biol.* **10**, 3365-3375.
**Novoa, I. and Carrasco, L.** (1999). Cleavage of eukaryotic translation initiation factor 4G by exogenously added hybrid proteins containing poliovirus 2Apro in HeLa cells: effects on gene expression. *Mol. Cell. Biol.* **19**, 2445-2454.
**Park, N., Katikaneni, P., Skern, T. and Gustin, K. E.** (2008). Differential targeting of nuclear pore complex proteins in poliovirus-infected cells. *J. Virol.* **82**, 1647-1655.
**Perales, C., Carrasco, L. and Ventoso, I.** (2003). Cleavage of eIF4G by HIV-1 protease: effects on translation. *FEBS Lett.* **533**, 89-94.
**Petersen, J. M., Her, L. S., Varvel, V., Lund, E. and Dahlberg, J. E.** (2000). The matrix protein of vesicular stomatitis virus inhibits nucleocytoplasmic transport when it is in the nucleus and associated with nuclear pore complexes. *Mol. Cell. Biol.* **20**, 8590-8601.
**Porter, F. W. and Palmenberg, A. C.** (2009). Leader-induced phosphorylation of nucleoporins correlates with nuclear trafficking inhibition by cardioviruses. *J. Virol.* **83**, 1941-1951.
**Porter, F. W., Bochkov, Y. A., Albee, A. J., Wiese, C. and Palmenberg, A. C.** (2006). A picornavirus protein interacts with Ran-GTPase and disrupts nucleocytoplasmic transport. *Proc. Natl. Acad. Sci. USA* **103**, 12417-12422.
**Pritchard, C. E., Fornerod, M., Kasper, L. H. and van Deursen, J. M.** (1999). RAE1 is a shuttling mRNA export factor that binds to a GLEBS-like NUP98 motif at the nuclear pore complex through multiple domains. *J. Cell Biol.* **145**, 237-254.
**Randall, R. E. and Goodbourn, S.** (2008). Interferons and viruses: an interplay between induction, signalling, antiviral responses and virus countermeasures. *J. Gen. Virol.* **89**, 1-47.
**Satterly, N., Tsai, P. L., van Deursen, J., Nussenzveig, D. R., Wang, Y., Faria, P. A., Levay, A., Levy, D. E. and Fontoura, B. M.** (2007). Influenza virus targets the mRNA export machinery and the nuclear pore complex. *Proc. Natl. Acad. Sci. USA* **104**, 1853-1858.
**Seipelt, J., Guarne, A., Bergmann, E., James, M., Sommergruber, W., Fita, I. and Skern, T.** (1999). The structures of picornaviral proteinases. *Virus Res.* **62**, 159-168.
**Terns, M. P. and Dahlberg, J. E.** (1994). Retention and 5′ cap trimethylation of U3 snRNA in the nucleus. *Science* **264**, 959-961.
**Ventoso, I., Barco, A. and Carrasco, L.** (1998). Mutational analysis of poliovirus 2Apro. Distinct inhibitory functions of 2apro on translation and transcription. *J. Biol. Chem.* **273**, 27960-27967.
**von Kobbe, C., van Deursen, J. M., Rodrigues, J. P., Sitterlin, D., Bachi, A., Wu, X., Wilm, M., Carmo-Fonseca, M. and Izaurralde, E.** (2000). Vesicular stomatitis virus matrix protein inhibits host cell gene expression by targeting the nucleoporin Nup98. *Mol. Cell* **6**, 1243-1252.
**Weidman, M. K., Sharma, R., Raychaudhuri, S., Kundu, P., Tsai, W. and Dasgupta, A.** (2003). The interaction of cytoplasmic RNA viruses with the nucleus. *Virus Res.* **95**, 75-85.